

# Efficient Quantum State Estimation with Over-complete Tomography

Chi Zhang,<sup>1</sup> Guo-Yong Xiang,<sup>1</sup> Yong-Sheng Zhang\*,<sup>1</sup> Chuan-Feng Li†,<sup>1</sup> and Guang-Can Guo<sup>1</sup>

<sup>1</sup>Key Laboratory of Quantum Information, University of Science and Technology of China, CAS, Hefei, 230026, P.R.China

(Dated: January 31, 2012)

It is widely accepted that the selection of measurement bases can affect the efficiency of quantum state estimation methods, precision of estimating an unknown state can be improved significantly by simply introduce a set of symmetrical measurement bases. Here we compare the efficiencies of estimations with different numbers of measurement bases by numerical simulation and experiment in optical system. The advantages of using a complete set of symmetrical measurement bases are illustrated more clearly.

PACS numbers: 03.67.-a, 03.65.Wj, 42.50.-p

## I. Introduction

Quantum states are the most important and fundamental elements in the quantum world. Because of the superposition property, quantum states are highly complex and difficult to identify. Quantum state tomography (QST) [1, 2], a universal method to reconstruct quantum states by making a series of measurements on an ensemble, plays an important role in quantum information science [3]. However, because of the asymmetrical distribution of the measurement bases of the early QST methods [1], all random errors (statistical or technological) [4] accumulate during the measurements so that the quantum state estimation is always inefficient [5]. Then a new symmetrical tomography scheme, called over-complete QST [6, 7], had been established. Its efficiency has been proven and it has been widely used in many experiments [8–14]. This method may find versatile usage in many fields, such as quantum computation and simulation [15, 16], quantum communication [3, 17], quantum metrology [18, 19], condensed matter physics [20], quantum chemistry [21, 22], and quantum biology [23, 24].

In this letter, first, we analyze and numerically simulate the quantum state estimation procedure and compare the efficiencies of over-complete QST with that of normal QST, then we experimentally demonstrate its efficiency in optical system.

## II. Numerical Simulation

Suppose that there are  $N$  copies of a quantum state, which is totally unknown before the measurements are made for the reconstruction task. An  $n$ -qubit quantum state can be described by a  $2^n$  dimensional density matrix [25]. Because the density matrix has the properties of normalization, Hermiticity, and positivity, it contains

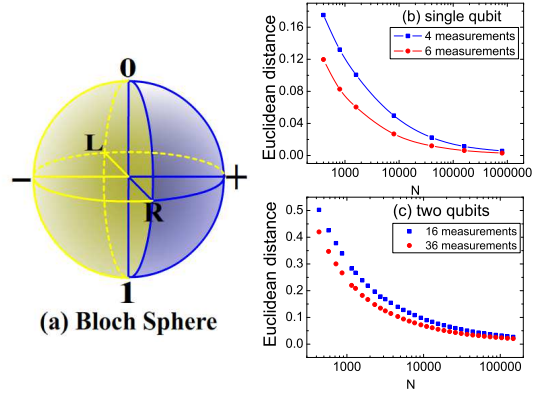


FIG. 1: (color online) Errors of over-complete QST and normal QST. (a). The measurement bases of over-complete QST (yellow and blue) are distributed symmetrically on the surface of the Bloch Sphere, while those of normal QST (blue) only cover a quarter of the surface. In (b) and (c), 1000 different states are chosen randomly from the entire state space. For each state, we simulate the tomography procedure with  $4^n$  (blue) and  $6^n$  (red) measurement bases for one qubit (b) and two qubits (c), where  $n$  is the number of qubits, with the same total resources  $N$ . We vary  $N$  approximately from  $10^2$  to  $10^6$ , and calculate the error of estimation by Euclidean distance for each chosen value of  $N$ . Each point represents the mean error of estimation for the 1000 states at each different  $N$ . One thousand samples are sufficient to draw the curve because the mean value and error bar do not change much between data volumes of 500 and 1000. It is obvious that over-complete QST is more precise.

$4^n - 1$  variables, so we need at least  $4^n$  measurements to determine the density matrix of the state. The standard QST method to reconstruct the density matrix is to equally divide the  $N$  copies into exactly  $4^n$  measurements, record the counts  $n_\nu$  for every measurement, and then apply maximum likelihood estimation (MLE) [1] to find the physical quantum state that is most likely to generate these measured data. To be specific, these measured data are assumed to be Gaussian distributed around the true values, so the probability of observing a

\*email: yshzhang@ustc.edu.cn

†email: cfli@ustc.edu.cn

particular set of counts is given by

$$P(n_1, \dots, n_m) = \frac{1}{N_{norm}} \exp\left[-\sum_{\nu=0}^m \frac{(\bar{n}_\nu - n_\nu)^2}{2\bar{n}_\nu}\right], \quad (1)$$

where  $N_{norm}$  is the normalization constant,  $m$  is the number of measurements, and  $\bar{n}_\nu = \frac{N}{m} \langle \psi_\nu | \hat{\rho} | \psi_\nu \rangle$  is the expectation value of  $|\psi_\nu\rangle$  measuring the state  $\hat{\rho}$ . Therefore, the physical density matrix with maximum  $P(n_1, \dots, n_m)$  is most likely to be the true state. This is a universally applicable method to estimate any previous unknown quantum states.

A serious problem of QST is that the selection of measurement bases is always asymmetric in the state space; in the Bloch Sphere [26] of a single qubit, for example, the four bases in early method cover only a quarter of the surface (Figure 1(a)). However, using the least possible number of measurement bases does not necessarily cost the minimum total resources. The real difficulties in experiments, such as the estimation of a quantum state of eight ions [27], are the limited resources, not the measurement times. According to previous study on the choice of measurement sets [28], inscribed Platonic solid of the Bloch sphere measurement sets result in the minimum error of estimation. This indicates that symmetrically arranged measurements will improve the precision significantly, in this letter, we provide insightful research on why the selection of measurement sets affects the precision and experimentally demonstrate this point. By numerical simulation of the tomography procedure on single-qubit and two-qubit states, it becomes clear that when these  $N$  copies are distributed equally into  $6^n$  symmetrical measurement bases, i.e., each measurement base receives  $N/6^n$  copies, the precision of the state estimation will be improved significantly. The chosen bases are of the form

$$|\psi\rangle = \otimes_{\nu=1}^n |\psi_\nu\rangle, \quad (2)$$

where  $|\psi_\nu\rangle \in \{|0\rangle, |1\rangle, |+\rangle, |-\rangle, |L\rangle, |R\rangle\}$ , with  $|\pm\rangle = \frac{1}{\sqrt{2}}(|0\rangle \pm |1\rangle)$ ,  $|L\rangle = \frac{1}{\sqrt{2}}(|0\rangle + i|1\rangle)$ ,  $|R\rangle = \frac{1}{\sqrt{2}}(|0\rangle - i|1\rangle)$ , which lie at the six polar symmetrical points of the Bloch Sphere (FIG. 1(a)). MLE is used to find the most likely density matrix, as in QST. The results are shown in FIG. 1 (b) and (c), wherein the error of estimation is represented by Euclidean distance  $\sqrt{\text{Tr}[(\rho - \hat{\rho})^2]}$  [3]. As can be seen from the figure, over-complete QST needs fewer resources than normal QST to reach the same precision.

In our work, the task of finding the minimum of likelihood function is efficiently executed by the simulated annealing algorithm [29], which proceeds as follows. (i). Start by estimating the target matrix,  $\hat{\rho}$ , as an arbitrary physical density matrix, such as the  $I/4$ , with an initial temperature  $T_0$ . (ii). Let the current temperature  $T$  decrease as the procedure continues, then transform the matrix to another one (for instance, change an element or partially transpose the matrix), and calculate the value of the likelihood function. The probability of accepting

the new  $\hat{\rho}$  depends on the ratio of the new and the old likelihood functions, and on the current temperature  $T$ ; more precisely, it is

$$\min\{\exp[-\frac{L(\hat{\rho}_{n+1}) - L(\hat{\rho}_n)}{kT_n}], 1\}, \quad (3)$$

where  $k$  is a constant number. (iii). Repeat step (ii) until the value of the likelihood function becomes stable. (iv). Report  $\hat{\rho}$  as the estimated density matrix. Analogous to the annealing process in solid state matter, the transition probability between two levels is determined by the temperature and the energy difference of the two levels. With  $T$  decreasing, the system will finally arrive at the ground state. In a similar way, the simulated annealing algorithm can find the minimum quickly and precisely.

First, we analyze the situation of single qubit. Finding the density matrix most likely to match the experimental data is very like the procedure of fitting a line with the least squares method [30]. Obviously, at least two points are needed to determine a line. To determine a line more accurately, we may measure each of the two points with more resources to make the measurements more reliable, or we may use a series of measurements and fit the line with more points. The latter approach is better, and it is therefore always used. The reason is that even though any single point is not so accurate, their statistical errors, which are random, will cancel each other. Moreover, if some types of random errors are related to the selection of the measurement bases, they will accumulate in the first method but cancel each other in the second. Especially when the measurement resources are distributed symmetrically, these errors will be expected to reduce to the minimum. In a similar way, when estimating an unknown quantum state, the statistical error is closely related to the count  $n_\nu$ , which is determined by the measurement base. Technological errors, such as the uncertainty on the angle of the wave plate, will also accumulate if there are only 4 measurement bases. Single qubit states can be described by points on the Bloch Sphere, and measurement bases can only lie on the surface. Therefore, the precision of estimation will be improved significantly if we use the six polar points, which are distributed symmetrically on the sphere, as measurement bases. In FIG. 1(a), these measurement bases can be regarded as 6 directions from which to observe the unknown states. Any particular set of 4 of them cannot reach a fine estimation because they cannot see the state from all directions (they cover only a quarter of the sphere), even though they are enough to determine the state in theory. For more than one qubit, the space of states grows exponentially, and we need to use the combination of these bases described by Eq. (2) to make up a complete set of symmetrical measurements.

In addition, to show more advantages of the over-complete QST method, we numerically simulate the estimation of concurrence [31], an important parameter in two-qubit entanglement verification [32]. It is defined as

$$C(\rho) = \max\{0, \lambda_1 - \lambda_2 - \lambda_3 - \lambda_4\}, \quad (4)$$

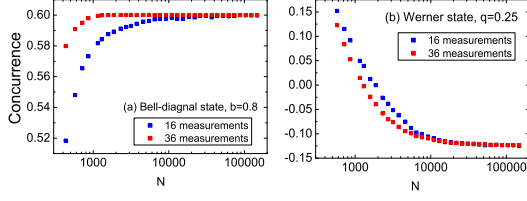


FIG. 2: (color online) Error of concurrence estimation. (a). Bell-diagonal state with  $b=0.8$ , the true concurrence is 0.6. (b). Werner state with  $q=0.25$ , the true concurrence is -0.125 (here we do not set its minimum value to zero).  $N$  is the total quantity of resources used for estimation. These two examples illustrate that over-complete QST is always closer to the true value than QST. We generate the curve with 300 samples for each point.

where  $\lambda_i$  are the eigenvalues, in decreasing order, of the Hermitian matrix  $R = \sqrt{\sqrt{\rho}\tilde{\rho}\sqrt{\rho}}$ , and  $\rho$  is the density matrix. Here we do not set its minimum value to zero so that we may study the estimation more clearly. Two common states, the Bell-diagonal state [33]

$$\rho = b|\psi^-\rangle\langle\psi^-| + (1-b)|\phi^-\rangle\langle\phi^-| \quad (5)$$

where  $|\psi^-\rangle = \frac{1}{\sqrt{2}}(|00\rangle - |11\rangle)$ ,  $|\phi^-\rangle = \frac{1}{\sqrt{2}}(|01\rangle - |10\rangle)$ , and the Werner state [34]

$$\rho = q|\psi^-\rangle\langle\psi^-| + (1-q)I/4 \quad (6)$$

are used as examples. The results are shown in FIG. 2. It is easy to see from the figure that the concurrence estimated by 36 measurements is closer to the true value than that estimated by 16 measurements. When data are insufficient, the deviation seems tremendous, the effect of which is caused by MLE [35]. Nonetheless, over-complete QST has reduced the deviation greatly. Consequently, the result from over-complete QST is more reliable than that obtained from normal QST, and over-complete QST is very useful to verify entanglement when resources are limited.

### III. Experimental Demonstration

Now it is clear that estimation by  $6^n$  measurements is better than that by  $4^n$ . Next, we experimentally demonstrate that a complete symmetrical set of measurement bases is the best choice for quantum state estimation. Taking two qubits as an example, here we conduct two all optical experiments on a Bell-diagonal state and a Werner state to find the optimal number of measurements for quantum state tomography. The experimental setup is described in FIG. 3, where the polarization  $|H\rangle$  and  $|V\rangle$  are used to represent  $|0\rangle$  and  $|1\rangle$ . Approximately  $2.5 \times 10^5$  photon pairs are used in total, which are divided equally into  $m = 16$  to  $m = 40$  measurement bases for tomography (see Table 1 for the selection order

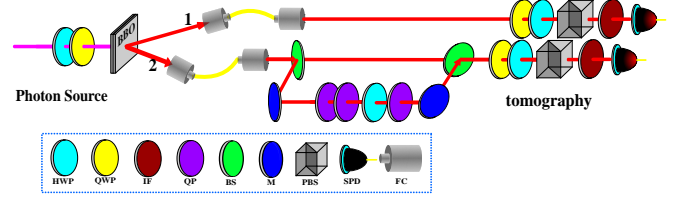


FIG. 3: (color online) Experimental setup. Here, the abbreviations of the components stand for the following: HWP – half wave plate, QWP – quarter wave plate, IF – interference filter, QP – long quartz plate, introducing complete dephasing between  $|H\rangle$  and  $|V\rangle$ , BS – beam splitter, M – mirror, PBS – polarizing beamsplitter, SPD – single photon detector, and FC – fiber coupler. An ultraviolet doubled femtosecond pulsed laser (about 100 mW, 390 nm, 76 MHz) is used to pump two BBO crystals for type I down conversion to generate entangled photon pairs ( $780 \text{ nm}$ ,  $\frac{1}{\sqrt{2}}(|HH\rangle - |VV\rangle)$ ), and the 2nd path is split into two branches, one of them is controlled by optical devices to prepare either a Bell-diagonal state with  $b = 0.8$  or a Werner state with  $q = 0.5$ . More precisely, we use an HWP to exchange  $|H\rangle$  and  $|V\rangle$  on the branch to prepare the Bell-diagonal state, while we use an HWP (transforming  $|H\rangle$  and  $|V\rangle$  to  $|+\rangle$  and  $|-\rangle$ , respectively) and QPs on the branch to prepare the Werner state. An attenuator is used to tune the ration  $q$  and  $b$ . The final state is detected by the automatic tomography system, which is controlled by a LabVIEW program and works precisely and efficiently.

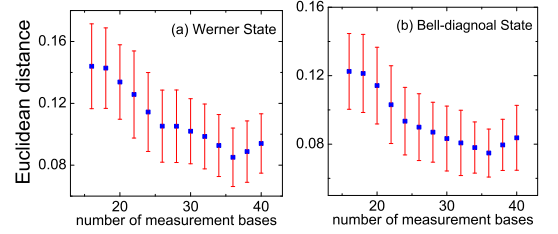


FIG. 4: (color online) Error of different numbers of measurement bases for  $N = 2.5 \times 10^5$ . (a). Werner state with  $q = 0.5$ , (b). Bell-diagonal state with  $b = 0.8$ . The  $x$ -axis shows the number of measurement bases; the  $y$ -axis shows the Euclidean distance. The state estimated from  $10^8$  data is regarded as the true one. We statistically calculate the mean value and standard deviation of the Euclidean distance from 60 individual experiments for each point, and we find that the mean value and standard deviation have already converged to certain values. For both states, the 36-base set is the best scheme.

of measurement bases). The results are shown in FIG. 4. They indicate that, among the tested sets of measurement bases, the set containing 36 bases (an over-complete symmetrical set), is the best; the others could not achieve such precision because they are not distributed symmetrically. This illustrates once more the importance of the choice of measurement bases.

In this experiment, the quantity of total resources is regarded as the sum of used resources for all measurement

bases. In fact, in many experiments [36], two orthogonal bases, such as  $|0\rangle$  and  $|1\rangle$ , were measured simultaneously because the PBS only separates them without degrading either one. In this way, the total amount of resources used by over-complete QST can be saved exponentially, and only  $3^n$  measurements are required. Normal QST, on the other hand, with its incomplete measurement bases, will waste part of these resources (it also needs at least  $3^n$  measurements). One caution is necessary here, however, saving resources in this way requires calibrating single photon detectors. Although a recent research [37] introduces a novel set of mutually unbiased bases for two qubits tomography, however, some of them are entangled states and require more complex setting to detect. An over-complete set of measurement bases in our experiment is easy to be realized in experiments and can be extended to more than two qubits system.

#### IV. Conclusion

In conclusion, we have made it clear that the precision of quantum state estimation is strongly affected by the selection of measurement bases. It has been proven that, when estimates are performed with the same quantity of

resources and the same estimation method (MLE), over-complete QST makes a great difference in improving the precision. Recently, several improved state estimation methods have been proposed, such as Bayesian mean estimation (BME) [38], hedged maximum likelihood estimation (HMLE) [39], compressed sensing method [40], and Marcus Cramer et al.'s method [41] for finitely correlated states (FCS) [42] or matrix product states (MPS) [43]. However, these methods can be only used in some special situations, that is, when the states are belong to some certain categories or prior assumption of the states are available. They have not revealed the intrinsic weakness of QST, the asymmetry distribution of the measurement bases. Remarkably, over-complete QST can be combined with these estimation methods to improve their efficiency significantly. We can also try other symmetrical measurement bases, such as the eight vertexes of the inscribed cube of the Bloch sphere. This choice of bases is similar to the bases of over-complete QST, and the result should also be very satisfactory.

#### Acknowledgment

This work was supported by the National Fundamental Research Program, and the National Natural Science Foundation of China (Grant Nos. 60921091, 10874162).

- 
- [1] D. F. V. James, P. G. Kwiat, W. J. Munro, and A. G. White, *Phys. Rev. A* **64**, 052312 (2001).
  - [2] K. Vogel, and H. Risken, *Phys. Rev. A* **40**, 2847-2849 (1989).
  - [3] M. A. Nielsen, and I. L. Chuang, *Quantum Computation and Quantum Information* (Cambridge University Press, Cambridge, England, 2000).
  - [4] C. E. Sarndal, B. Swenson, and J. Wretman, *Model Assisted Survey Sampling*, Springer-Verlag. (1992).
  - [5] W. K. Wootters and B. D. Fields, *Annals of Physics* **191**, 363 (1989).
  - [6] R. Kaltenbaek, J. Lavoie, B. Zeng, S. D. Bartlett and K. J. Resch, *Nature Physics*, **6**, 850 (2010).
  - [7] N. K. Langford, T. J. Weinhold, R. Prevedel, K. J. Resch, A. Gilchrist, J. L. O'Brien, G. J. Pryde, and A. G. White, *Phys. Rev. Lett.* **95**, 210504 (2005).
  - [8] R.B.A. Adamson and A.M. Steinberg, *Phys. Rev. Lett.* **105**, 030406 (2010).
  - [9] S. Olmschenk, D. N. Matsukevich, P. Maunz, D. Hayes, L. M. Duan and C. Monroe, *Science*, **323**, 486 (2009).
  - [10] G. Lima, L. Neves, R. Guzman, E. S. Gomez, W. A. T. Nogueira, A. Delgado, A. Vargas, and C. Saavedra, *Optics Express*, **19**, 3542 (2011).
  - [11] N. Kiesel, C. Schmid, G. Toth, E. Solano, and H. Weinfurter, *Phys. Rev. Lett.* **98**, 063604 (2007).
  - [12] W. Wieczorek, R. Krischek, N. Kiesel, P. Michelberger, G. Toth, and H. Weinfurter, *Phys. Rev. Lett.* **103**, 020504 (2009).
  - [13] K. Dobek, M. Karpinski, R. Demkowicz-Dobrzanski, K. Banaszek and P. Horodecki, *Phys. Rev. Lett.* **106**, 030501 (2011).
  - [14] Y. I. Bogdanov, G. Brida, M. Genovese, S. P. Kulik, E. V. Moreva, and A. P. Shurupov, *Phys. Rev. Lett.* **105**, 010404 (2010).
  - [15] D. P. DiVincenzo, *Science* **270**, 255 (1995).
  - [16] R. P. Feynman, *International Journal of Theoretical Physics* **21**, 467 (1982).
  - [17] C. H. Bennett, G. Brassard, C. Crepeau, R. Jozsa, A. Peres, and W. K. Wootters, *Phys. Rev. Lett.* **70**, 1895-1899 (1993).
  - [18] V. Giovannetti, S. Lloyd, and L. Maccone, *Phys. Rev. Lett.* **96**, 010401 (2006).
  - [19] B. M. Escher, R. L. de Matos Filho, and L. Davidovich, *Nature Physics* **7**, 406 (2011).
  - [20] P. Hauke, *New Journal of Physics* **12**, 113037 (2010).
  - [21] B. P. Lanyon, J. D. Whitfield, G. G. Gillett, M. E. Goggin, M. P. Almeida, I. Kassal, J. D. Biamonte, M. Mohseni, B. J. Powell, M. Barbieri, A. Aspuru-Guzik, A. G. White, *Nature Chemistry* **2**, 106 (2010).
  - [22] A. Szabo and S. O. Neil, *Modern Quantum Chemistry: Introduction to Advanced Electronic Structure Theory* (1996).
  - [23] P. Ball, *Nature* **474**, 272 (2011).
  - [24] W. G. Cooper, *BioSystems* **97**, 73-89 (2009).
  - [25] U. Fano, *Reviews of Modern Physics* **29**, 74-93 (1957).
  - [26] S. Frank, *Linearity, symmetry, and prediction in the Hydrogen atom*. New York: Springer. ISBN 0-387-24637-1 (2005).
  - [27] H. Hffner, W. Hnsel, C. F. Roos, J. Benhelm, D. Chek-al-kar, M. Chwalla, T. Krber, U. D. Rapol, M. Riebe, P. O. Schmidt, C. Becher, O. Guhne, W. Dur and R. Blatt, *Nature* **438**, 643 (2005).
  - [28] M. D. de Burgh, N. K. Langford, A. C. Doherty and A.

- Gilchrist, *Phys. Rev. A* **78**, 052122 (2008).
- [29] S. Kirkpatrick, C. D. Gelatt, and M. P. Vecchi, *Science* **220**, 671 (1983).
- [30] S. M. Stigler, *The History of Statistics: The Measurement of Uncertainty Before 1900*. Cambridge, Belknap Press of Harvard University (1986).
- [31] V. Dananic and A. Bjelis, *Phys. Rev. Lett.* **80**, 10-13 (1998).
- [32] S. J. van Enk, N. Lutkenhaus and H. J. Kimble, *Phys. Rev. A* **75**, 052318 (2007).
- [33] F. Verstraete, J. Dehaene and B. DeMoor, *Phys. Rev. A* **64**, 010101(R) (2001).
- [34] R. F. Werner, *Phys. Rev. A* **40**, 4277 (1989).
- [35] J. O. S. Yin and S. J. van Enk, arXiv:1011.2709v2
- [36] G. Toth, W. Wiecezorek, D. Gross, R. Krischek, C. Schwemmer, H. Weinfurter, arXiv:1005.3313v4
- [37] R. B. A. Adamson, and A. M. Steinberg, *Phys. Rev. Lett.* **105**, 030406 (2010).
- [38] R. Blume-Kohout, *New J. Phys.* **12**, 043034 (2010).
- [39] R. Blume-Kohout, *Phys. Rev. Lett.* **105**, 200504 (2010).
- [40] D. Gross, Y. K. Liu, S. T. Flammia, S. Becker and J. Eisert, *Phys. Rev. Lett.* **105**, 150401 (2010).
- [41] M. Cramer, M. B. Plenio, S. T. Flammia, R. Somma, D. Gross, S. D. Bartlett, O. L. Cardinal, D. Poulin and Y. K. Liu, *Nature Communications* **1**, 149 (2010).
- [42] M. Fannes, B. Nachtergaele and R. F. Werner, *Comm. Math. Phys.* **144**, 443-430 (1992).
- [43] D. Perez-Garcia, F. Verstraete, M. M. Wolf and J. I. Cirac, *Quant. Inf. Comp.* **7**, 401-430 (2007).

TABLE I: CQST measurement bases selected for both experiments and simulations. Here,  $|L\rangle = \frac{1}{\sqrt{2}}(|H\rangle + i|V\rangle)$ ,  $|R\rangle = \frac{1}{\sqrt{2}}(|H\rangle - i|V\rangle)$ ,  $|+\rangle = \frac{1}{\sqrt{2}}(|H\rangle + |V\rangle)$ , and  $|-\rangle = \frac{1}{\sqrt{2}}(|H\rangle - |V\rangle)$ .

$\nu$	measurement base	$\nu$	measurement base
1	$ HH\rangle$	2	$ HV\rangle$
3	$ VH\rangle$	4	$ VV\rangle$
5	$ RH\rangle$	6	$ RV\rangle$
7	$ +V\rangle$	8	$ +H\rangle$
9	$ +R\rangle$	10	$ ++\rangle$
11	$ R+\rangle$	12	$ H+\rangle$
13	$ V+\rangle$	14	$ VL\rangle$
15	$ HL\rangle$	16	$ RL\rangle$
17	$ LL\rangle$	18	$  - L\rangle$
19	$  - +\rangle$	20	$  - -\rangle$
21	$ + -\rangle$	22	$ L+\rangle$
23	$ LR\rangle$	24	$  - R\rangle$
25	$ HR\rangle$	26	$ VR\rangle$
27	$ RR\rangle$	28	$ +L\rangle$
29	$  - H\rangle$	30	$  - V\rangle$
31	$ LH\rangle$	32	$ LV\rangle$
33	$ H+\rangle$	34	$ V+\rangle$
35	$ L+\rangle$	36	$ R+\rangle$